R. & M. No. 2264
(9241)
A.R.C. Technical Report

MINISTRY OF SUPPLY

AERONAUTICAL RESEARCH COUNCIL
REPORTS AND MEMORANDA

Flight Tests at High Mach Number on E 28/39 W4041 (Single-engined Jet-propelled Aircraft)

By

A. W. Thom, B.A., F. Smith, M.A., and J. Brotherton

LONDON : HIS MAJESTY'S STATIONERY OFFICE
1948
Price 3*s.* 0*d.* net

Flight Tests at High Mach Number on E 28/39 W 4041 (Single-engined Jet-propelled Aircraft)

By

A. W. Thom, B.A., F. Smith, M.A. and J. Brotherton

Communicated by the Principal Director of Scientific Research (Air), Ministry of Supply

Reports and Memoranda No. 2264
October, 1945*

Summary.—This report describes flight tests at Mach numbers up to 0·816 on the E 28/39 W 4041, the first jet-propelled aircraft to be flown in this country. For these tests the aircraft was fitted with wings of "high-speed" section (EC 1240/0640). Alternative wings of conventional section (NACA 23012) were also available; it was intended to repeat the tests with these wings, but before this could be done the aircraft was required for other purposes.

Measurements of incidence, aileron and elevator angles, stick force and aircraft drag were made. In addition, measurements of pressure distribution were made at a section of the wing, and the profile drag of the same wing section was measured by the "pitot comb" method. The results showed that, as the Mach number increased above about 0·75, there was a large nosedown trim change and an increase of drag. For a given Mach number, both these effects were found to be more serious on this aircraft than on a Spitfire, suggesting that this "high-speed" type of section (EC 1240/0640) may be less suitable for flight at high Mach numbers than the conventional section (NACA 2212) of the Spitfire.

A pronounced "hysteresis" effect was observed in the wing pressure distributions at high Mach numbers, leading to different results for increasing and decreasing Mach number, at the same Mach number and lift coefficient. This apparent "hysteresis" has not been explained and no corresponding effect was found in the profile drag measurements.

1. *Introduction.*—As part of the programme of flight tests at the Royal Aircraft Establishment to investigate phenomena at speeds approaching the speed of sound it was desired to test an aircraft free from nacelles and propeller difficulties at high Mach number. The jet-propelled E 28/39 W 4041 was ideal for this work, having a single jet propulsion unit installed in the fuselage with the air intake at the nose of the fuselage. The wings were thus free from interference.

For these tests the aircraft was fitted with wings of EC 1240/0640 section tapering from 12·5 per cent. thickness-chord ratio at the root to 10 per cent. at the tip. This "high-speed" section was specially designed for this aircraft to have a flat-topped velocity distribution giving minimum excess velocities over the surface. Surface pressure plotting holes were fitted on a test section of the starboard wing. The profile drag of this section was also measured by the "pitot-comb" method and overall drag of the aircraft measured by means of a longitudinal accelerometer[1].

Tests were made up to a Mach number of 0·72 when a longitudinal pitching oscillation of the aircraft developed. This oscillation was cured and the tests continued up to $M = 0{\cdot}816$, the maximum reached during these tests, in which condition the aircraft became extremely difficult to handle, due to buffeting and general oscillations about all three flight axes.

Investigations of the causes of the buffeting by means of deep tufting on the wing root, tailplane–fuselage junction and on the fuselage nose were begun. It was intended to follow up this work by a series of tests on the aircraft with wings of conventional section (NACA 23012), for which wings were available; the intention was to give a direct comparison between the two types of section. Before this could be done, however, the tests were terminated as the aircraft was required for exhibition purposes.

*R.A.E. Report No. Aero. 2086 received 17th December, 1945.

2. *Description of Tests.*—2.1. *Aircraft.*—The E 28/39 W 4041 aircraft (Fig. 1) was the first jet-propelled aeroplane to be flown in this country and was designed for engine test-bed work. It is, however, of very clean aerodynamic design and was chosen as being suitable for high Mach number work. In addition the aircraft has two alternative sets of wings, one with NACA 23012 profile and the other with EC 1240/0640 " high-speed " design profile.

A test section was chosen for investigation of pressure distribution and profile drag 81 inches from the aircraft centre-line on the starboard wing (Figs. 2 and 3). Thirty positions for measurement of the surface pressure were used (Fig. 3), and a pitot comb was fixed 10 inches aft of the trailing edge. Further details are given in Table 1.

For these tests the ailerons and elevator, normally fabric covered, were metal covered since buffeting and elevator trim change were anticipated.

With the co-operation of Power Jets, Ltd., a W 2/700 jet propulsion unit was installed; structural limitations at the rear end of the fuselage limited the size of jet pipe that could be used and thus the maximum thrust of the engine. Engine test results have been described in a separate note[2].

2.2. *Instrumentation.*—Owing to the small size of the aircraft and the small amount of space available for an automatic observer the instrumentation of the aircraft presented quite a difficult problem.

The aircraft was fitted with an incidence vane on the starboard wing 60 per cent. of the local wing chord forward of the leading edge. The standard pitot-static head occupied the corresponding position on the port wing. The positions of both the ailerons and the elevator and the values of stick force were recorded by means of remote reading desynn indicators. The following engine data was recorded: jet pipe temperature, jet pipe pitot head, compressor delivery temperature, compressor delivery pressure, r.p.m., intake pressure and temperature. The aircraft instruments fitted were: aircraft altimeter, lag altimeter (connected to the aircraft altimeter by a length of calibrated fine bore tubing to represent lag in the aircraft tubing), aircraft airspeed indicator, 5 desynn receivers, normal accelerometer and longitudinal accelerometer. For measuring the test section profile drag 25 airspeed indicators were fitted and these were replaced by 30 airspeed indicators for the pressure distribution tests.

All these instruments were accommodated on three instrument panels (Fig. 4) which were mounted mutually at right angles to one another in the radio compartment. The radio compartment is situated under the pilot's seat and is reached through the nose wheel undercarriage doors.

The starboard and aft panels were each photographed by two robot cameras and the bottom panel by one camera placed under the panel photographing the panel through a mirror placed above the panel. A sixth camera was later installed in a fairing on the port wing tip to photograph wing root tufts.

All cameras were operated simultaneously at about two-second intervals by a T.35 camera control. The results given by the separate cameras were matched by means of veeder counters operated by an independent thermostatically controlled clock, which also supplied the time base necessary for the analysis of the results. Electric buzzers were attached to each panel to ensure ample vibration and to avoid error in instrument readings due to the lack of vibration in a jet-propelled aircraft. These buzzers were operated by the T.35 control about $\frac{1}{4}$ of a second before photographs were taken. The T.35 control was started by the pilot, and he was supplied with an indicator to show that the system was in operation.

2.3. *Tests.*—The aircraft position error was obtained by measuring the apparent air pressure given by the static tube in flight at low altitude. The true pressure was calculated from the ground air pressure and a ground observation of the true aircraft height. The results together with the compressibility corrections assumed are shown in Fig. 5.

A few tests were made at 10,000 ft. altitude and 300 to 400 m.p.h. I.A.S. to establish the aircraft characteristics at low Mach number. The high Mach number dives were then commenced. The usual technique was to climb the aircraft to 37,000 to 40,000 ft. and then dive at a steady angle until the maximum Mach number desired for the particular test was reached. The aircraft was then pulled out of the dive with 2 to 3g normal acceleration. Owing to the limited film in the cameras the pilot switched on the T.35 control at about $0 \cdot 1$ Mach number less than the maximum to be attained. The cameras then gave a complete record from a Mach number $0 \cdot 1$ less than the maximum to the maximum and then back to the initial Mach number. In this way the aircraft characteristics for both increasing and decreasing Mach number were obtained.

The aircraft was not fitted with an elevator trimmer but only with small metal tabs which could be adjusted on the ground. Accordingly to relieve the pilot of strain during the climb these tabs were set to trim the aircraft hands off at about 250 m.p.h. I.A.S. As a result the stick forces at high I.A.S. were fairly large.

Dives were started with a maximum Mach number of $0 \cdot 65$ and this maximum steadily increased in subsequent dives. At $M = 0 \cdot 72$ a longitudinal pitching oscillation of about one second period developed and could not be stopped by the pilot. On one flight oscillations of normal acceleration from 0 to 4g were noted by the pilot from this cause.

The pilot reported uncontrollable motion of the elevator during the oscillation. This, together with the fact that it had not been reported in previous tests with fabric-covered elevators, suggested the elevators as a possible cause of the trouble. They are convex in form, following the EC 1240 section of the tailplane with a trailing edge angle of 20 deg. It was thus possible that the elevator characteristics, although satisfactory at low Mach number, changed with Mach number in such a manner as to give a longitudinal hunting essentially similar to the directional " snaking " associated with convex or horn-balanced rudders with positive b_1. Accordingly the remedy usually applied for directional snaking was tried ; one foot of $\frac{3}{16}$ in. cord was attached to each side of the trailing edge of the elevator on top and bottom surface. This cured the oscillation up to $M = 0 \cdot 80$ where the pilot again reported an incipient oscillation. The amount of cord was doubled and no further oscillations were reported. The stick forces were increased as a result of this modification but since the aircraft is very light on its controls this increase in stick force was not troublesome.

The tests were continued up to $M = 0 \cdot 816$ where the pilot reported buffeting and general yawing, pitching, and rolling of the aircraft. The Mach number was not increased further and investigation of the buffeting by means of tufts was begun.

At this stage the automatic observer was changed from recording section profile drag to recording section pressure distribution.

3. *Results*.—3.1. *Aileron Movement*.—The position of the ailerons was recorded by desynn recorders in level flight and in the dive. From these results the aileron downfloat and the aileron movement applied by the pilot to maintain level flight have been obtained and plotted as a function of Mach number (Figs. 7 and 8). There is a noticeable Mach number effect on both aileron downfloat and pilot's movement both of which would tend to produce wing distortion at high Mach numbers.

3.2. *Incidence*.—The incidence vane was fitted well outboard on the starboard wing and, in fact, records the incidence of the wing at this section. Since there is considerable aileron movement with Mach number producing wing twist the incidence recorded will not relate directly to the mean aircraft lift coefficient. The vane will, however, record main changes in the lift coefficient-incidence relation. The results have been analysed in the form of change of incidence from low Mach number as a function of Mach number and have been interpolated at fixed values of aircraft coefficient, namely $C_L = 0 \cdot 05$, $0 \cdot 10$ and $0 \cdot 15$ (Fig. 9). As the Mach number increases to $0 \cdot 78$ the incidence decreases noticeably due to aileron effect on wing distortion and the spread of high top surface suctions from the wing root outboard towards the tip. Above $M = 0 \cdot 78$ the incidence rises rapidly corresponding to the development of the shock wave (*see* section 3.5) on the upper and lower surfaces of the wing.

3.3. *Trim Change.*—The change in elevator angle with Mach number is shown in Fig. 10. The results have been interpolated to fixed values of normal acceleration. The usual nose-down trim change is apparent here, and, in fact, is one of the largest yet measured. Due to the small size of the aircraft it was, however, possible for the pilot to hold these large changes of elevator angle.

3.4. *Stick Force.*—The values of stick force obtained during the tests have been reduced to those corresponding to 400 m.p.h. E.A.S. for ease of comparison and interpolated to fixed values of normal acceleration (Fig. 11). It must be borne in mind that there is no elevator trim tab on this aircraft and with the fixed trimmers adjusted for 250 m.p.h. E.A.S. a push of some 30 lb. was required at 400 m.p.h. E.A.S. at low Mach numbers. The stick force changed rapidly with Mach number, corresponding to the large trim change of Fig. 10, and reached a maximum pull of nearly 60 lb. in the pull-out at $M = 0 \cdot 81$.

3.5. *Profile Drag.*—The section profile drag was deduced from analysis of the curves of pitot head loss given by the pitot comb behind the test section ; the method is described in Ref. 3. The section profile drag values obtained in level flight are shown in Fig. 12 together with the theoretical values[4] for transition at leading edge and 20 per cent. chord. The flight values correspond to transition at 10 per cent. to 20 per cent. chord, a position which corresponds well with pressure distribution over the section (Fig. 18).

The normal " top-hat " curves of pitot head loss were obtained from the pitot comb readings up to $M = 0 \cdot 75$. Here a loss of head outside the " top-hat " curve developed, corresponding to the appearance of a shock wave on the top surface. At $M = 0 \cdot 77$ a similar loss developed on the lower part of the pitot comb corresponding to a shock wave on the lower surface. At $M = 0 \cdot 78$ and $0 \cdot 81$ these losses spread outside the pitot comb (length $0 \cdot 26c$) on top and bottom surfaces respectively and thus the total profile drag was not recorded. The results of these measurements are given in Figs. 13 and 14. Fig. 13 shows the profile drag excluding the shock wave drag and Fig. 14 shows the profile drag including the shock wave drag as measured by the comb but it should be remembered that above $M = 0 \cdot 78$ this is not the total shock wave drag.

The aircraft drag was obtained from readings of the longitudinal accelerometer[1] and engine thrust in flight. The induced drag was deduced from analysis of the drag results and found to be 10 per cent. greater than the theroretical value for elliptic distribution. The overall aircraft profile drag coefficient is shown in Fig. 15 ; the drag begins to rise at $M = 0 \cdot 71$. The section profile drag and the aircraft profile drag are shown comparatively in Fig. 16. Since the drag rise will start at a lower Mach number in the wing root than at the test section, the curves indicate that practically all the drag rise of the aircraft is attributable to the wings.

3.6. *Tufting the Wing Root.*—To examine the drag rise in the wing root and find the cause of the buffeting, reported by the pilot, tufts were attached to the surface of the port wing root and photographed by a camera on the port wing tip. Contrary to expectation no major breakaway at high Mach numbers was observed (Fig. 17). There was however a breakaway behind the shallow blister on the top surface of the wing above the undercarriage bay (Fig. 1), which may account for the buffeting. It was hoped to continue this examination with tufts in the tailplane–fuselage junction and tufts around the air intake at the nose of the fuselage since a relatively small breakaway in these positions might produce appreciable buffeting. The tests, however, had to be discontinued at this stage.

3.7. *Pressure Distribution.*—Static pressures were measured around the test section at thirty positions for Mach numbers from $0 \cdot 68$ to $0 \cdot 816$ and back to $0 \cdot 68$. Typical curves of pressure coefficients around the section are shown for increasing and decreasing Mach numbers and for a typical low Mach number in Fig. 18. The development of the shock waves on upper and lower surface can clearly be seen and correspond to the pitot comb shock wave losses discussed in section 3.5.

Typical positions around the part of the wing surface over which the shock waves develop have been taken and the pressure coefficients plotted for these positions against Mach number (Fig. 19). These figures show a definite hysteresis loop in the pressure coefficient with increasing and decreasing Mach number, the value for decreasing Mach number always being the lower. This loop is very pronounced on the bottom surface of the wing.

Using these figures the pressure coefficient distributions around the surface have been interpolated for four typical Mach numbers both increasing and decreasing (Fig. 22). These show clearly the different form of the shock wave for increasing and decreasing Mach numbers. The shock wave on the top surface for decreasing Mach number appears to lag behind that for increasing Mach number thus giving a larger hump in the pressure distribution curve for the same Mach number.

The shock wave on the bottom surface seems to develop quite slowly with increasing Mach number, starting at about 40 per cent. chord and moving back to 65 per cent. chord. With decreasing Mach number the decay of the shock again appears to lag and in addition the shock wave divides into two, one staying at 65 per cent. and the other moving forward to 40 per cent.

The suctions at $M = 0 \cdot 81$ are appreciably higher than those measured on the Spitfire[5] with a conventional section of about the same thickness-chord ratio.

It might be expected that the hysteresis phenomena of the shock wave might give rise to a hysteresis loop in the profile drag curve (Figs. 13 and 14). This hysteresis is not apparent and, if present, lies within the scatter of the experimental points.

3.8. *Test Section Lift Coefficient.*—The variations of section lift coefficient and aircraft lift coefficient with Mach number on a typical flight are shown in Fig. 20. The difference between the lift coefficients is given in Fig. 21 as a function of Mach number. It will be seen that as the shock wave develops in the wing root with the attendant loss of lift and spreads outboard with increasing Mach number, an increasing proportion of the aircraft lift is carried by the wing near the test section. At $M = 0 \cdot 80$, however, the lift loss has spread out as far as the test section, which suddenly carries less of the total lift once more, and by $M = 0 \cdot 815$ this part of the wing is again carrying its normal proportion of the lift.

4. *Conclusions.*—The results of these tests have incidated several important conclusions that can be drawn about wing sections of " high-speed " design. The elevator trim change and the stick forces accompanying the trim change are much larger than for the Spitfire XI. Explorations of the test section suggest that these increases can be partly attributed to the " flat-top " pressure distribution of the wing section. The rise in profile drag is similarly much greater than that of the Spitfire XI[6] at the same Mach number.* It appears that this rise in drag is not attributable to any major breakaway in the wing root and the pitot comb results similarly show no large drag increase coming from the " top-hat " part of the traverse (Fig. 13). In fact the pitot comb indicates that the rapid increase in drag is caused by large shock wave losses on both wing surfaces.

The test section pressure distribution also incidates the development of powerful shock waves on both surfaces, the pressure coefficients at $M = 0 \cdot 81$ being greater than those recorded on Spitfire XI in spite of the initial " flat-top " distribution at low Mach numbers.

The tests appear to confirm recent information of wind-tunnel tests in Germany where it was shown that " high-speed " design profiles, although having a higher critical Mach number, nevertheless have much more rapid increases in drag above this Mach number than a section of conventional design.

It would obviously have been of great advantage to repeat the tests on this aircraft with the alternative wings of conventional design but this is unfortunately no longer possible.

---

*1947. More recent tests on a Spitfire XXI, considered to be more reliable than that described in Ref. 6, show the increase in drag of Spitfire with Mach number to be more serious than indicated in that report, the profile drag coefficient at $M = 0 \cdot 86$ reaching a value of $0 \cdot 051$ compared with $0 \cdot 038$ of Ref. 6. This rise of drag is still less rapid than for E 28/39, although bearing in mind the differences in wing mean thickness-chord ratio between the two aircraft (Spitfire $= 0 \cdot 10$ and E 28/39 $= 0 \cdot 12$). The two results are now more consistent.

REFERENCES

No.	Author	Title, etc.
1	F. Smith and A. W. Thom	Note on the Use of a Longitudinal Accelerometer for Measuring Aircraft Drag in Flight in the Dive. R.A.E. Tech. Note No. Aero. 1649. June, 1945. (Unpublished).
2	D. H. Whaley and A. W. Thom ..	Note on Flight Tests of the W2/700 No. 10 Turbine Engine in the E 28/39 Aircraft. R.A.E. Tech. Note No. Aero. 1536. A.R.C. 8326. October, 1944. (Unpublished).
3	J. S. Thompson	A Simple Method of Computing C_D from Wake Traverses at High Speeds. R.A.E. Report No. Aero. 2005. A.R.C. 8462. January, 1945. (Unpublished).
4	N. E. Winterbottom and H. B. Squire	Note on Further Wing Profile Drag Calculations. R.A.E. Report No. BA.1634. October, 1940. A.R.C. 4871. Addendum to R. & M. 1838.
5	W. J. Charnley and W. Mair	Measurements of Pressure Distribution on a Spitfire Wing in Flight at High Speeds. R. & M. 2160. August, 1945.
6	R. Smelt, W. J. Charnley and R. Rose	Drag and Trim Changes on Spitfire, Mustang and Thunderbolt in Flight at High Mach Numbers. R.A.E. Report No. Aero. 1903 A.R.C. 7424. January, 1944. (Unpublished).

TABLE 1

Aircraft Data

Aircraft all-up weight	4,481 lb.
Wing area	148 sq. ft.
Wing section	EC 1240/0640
Wing thickness/chord ratio at root and at tip	0·125, 0·100
Static stability margin at low Mach number	0·03 A.M.C.
Distance of test section from aircraft centre-line	81 inches
Test section thickness/chord ratio	0·117
Test section chord	64·3 inches
Pitot comb length	16·5 inches
Pitot comb distance aft of trailing edge	10 inches

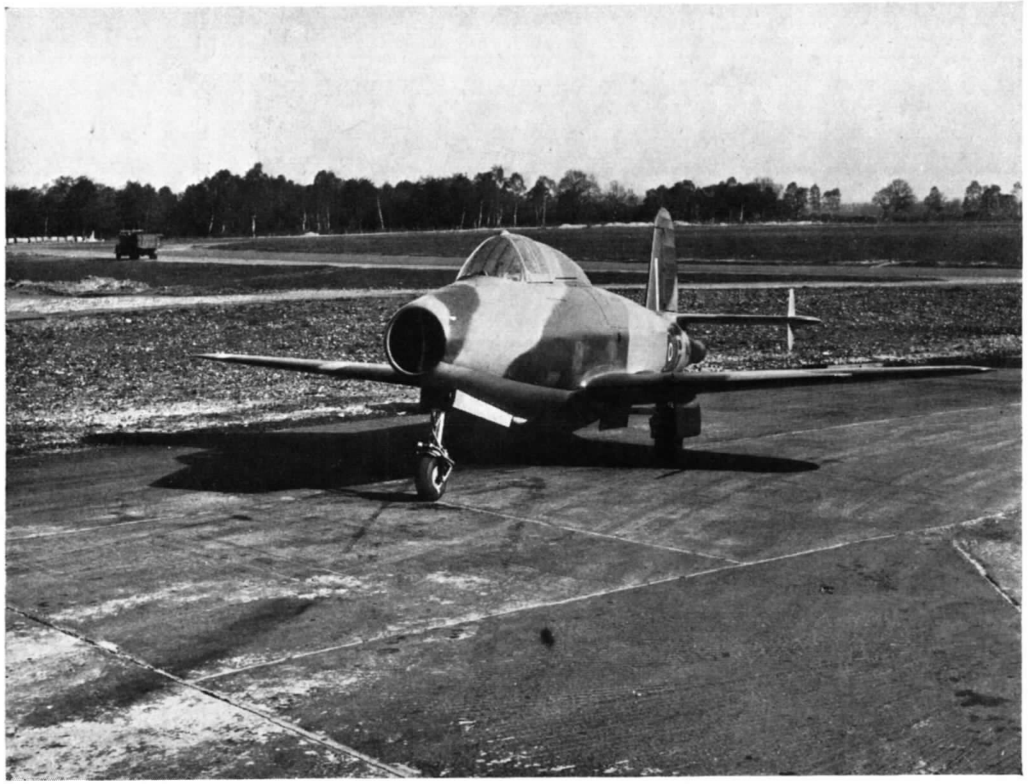

FIG. 1. E 28/39 W 4041

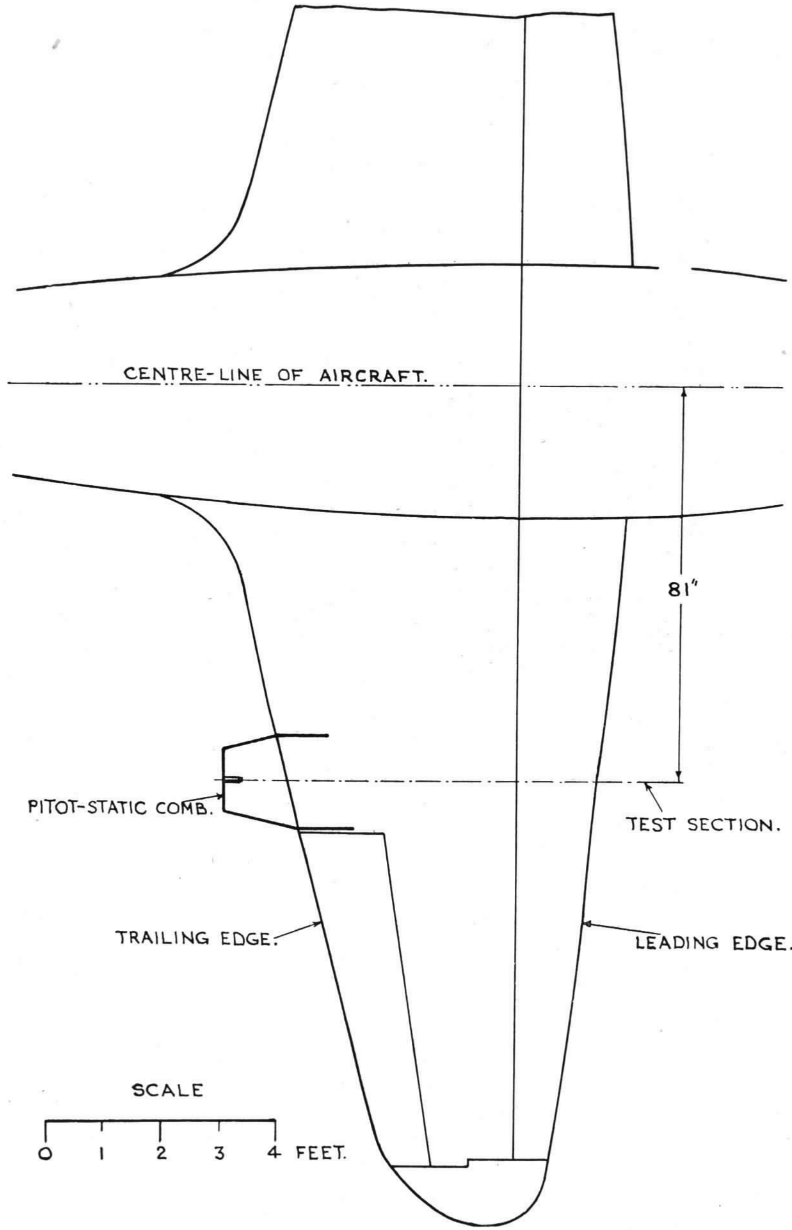

FIG. 2. Plan of Wing Showing Test Section.

(8630)
A*

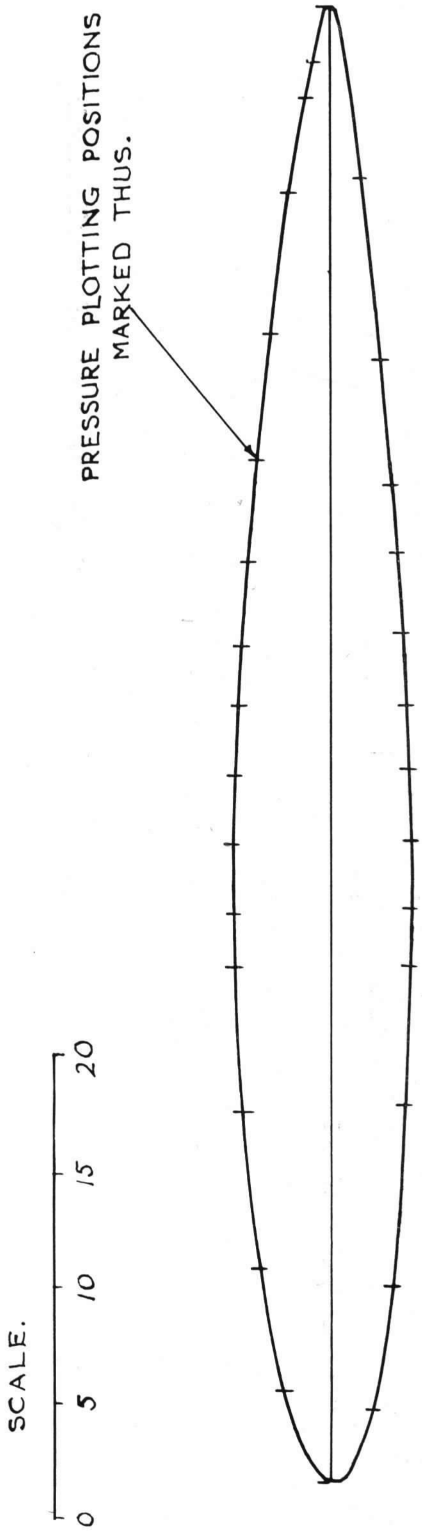

TEST SECTION CHORD = 64·3 INS.
TEST SECTION MAXIMUM THICKNESS = 11·7% CHORD AT 41% CHORD.

FIG. 3. Test Section Profile.

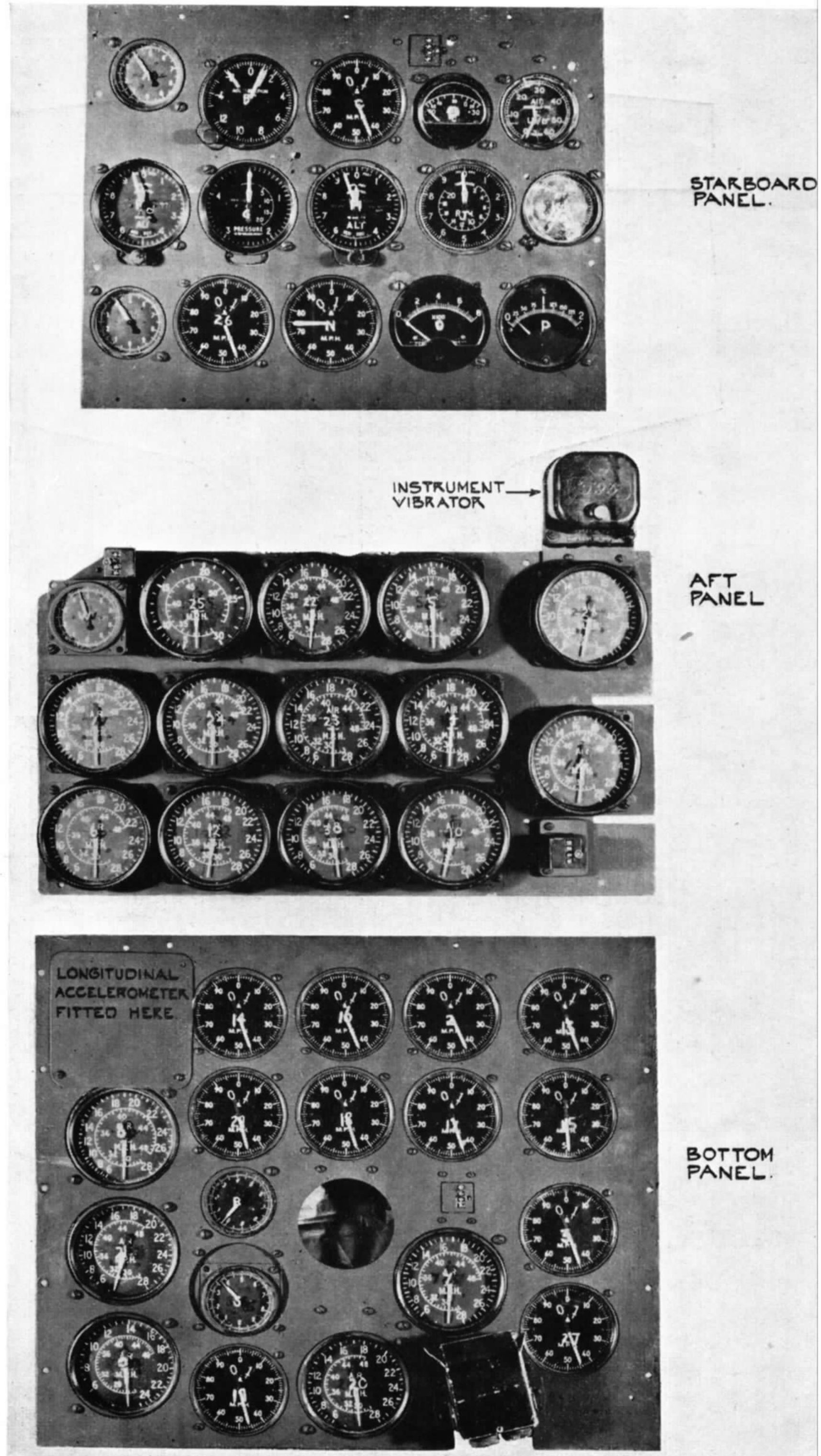

FIG. 4. Automatic Observer.

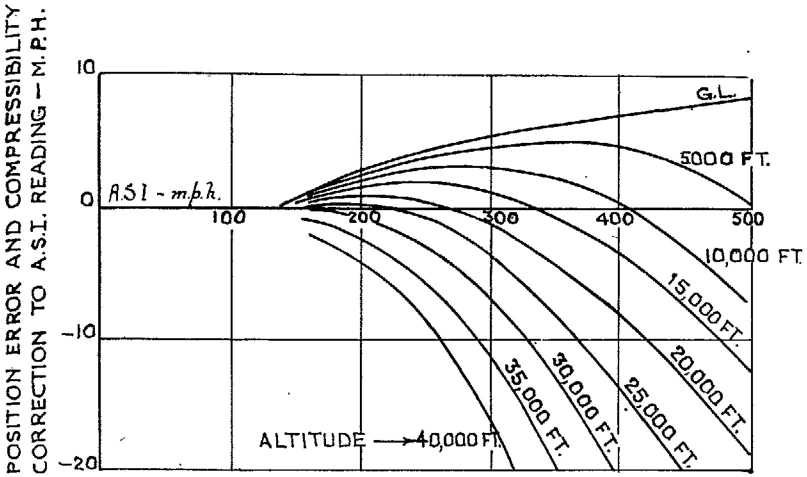

FIG. 5. Correction to A.S.I. Reading.

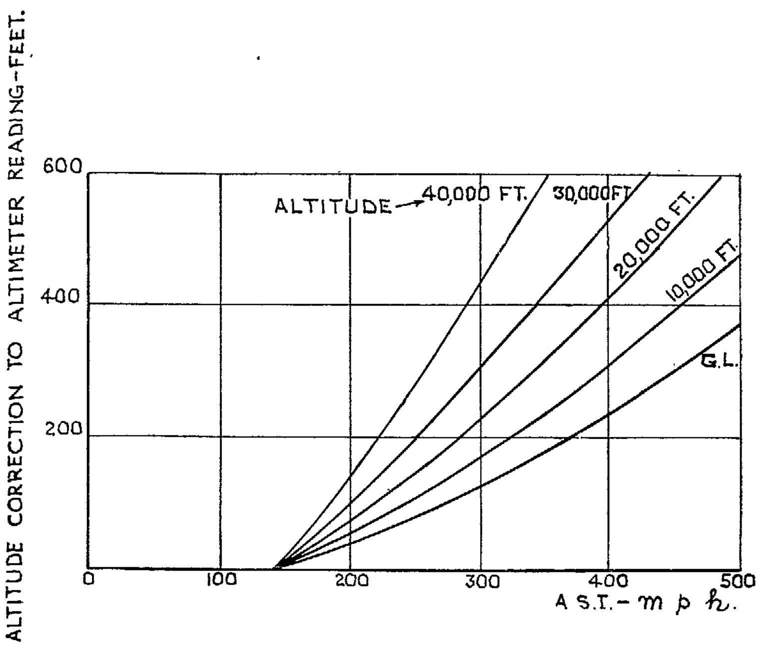

FIG. 6. Correction to Altimeter Reading.

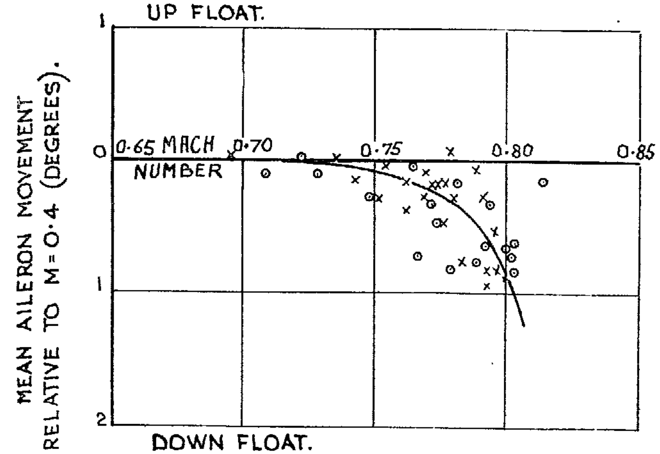

FIG. 7. Aileron Down Float.

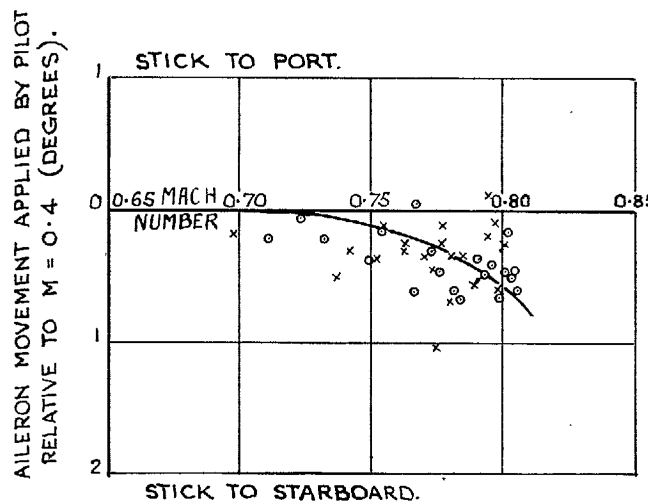

FIG. 8. Aileron Movement Applied by Pilot.

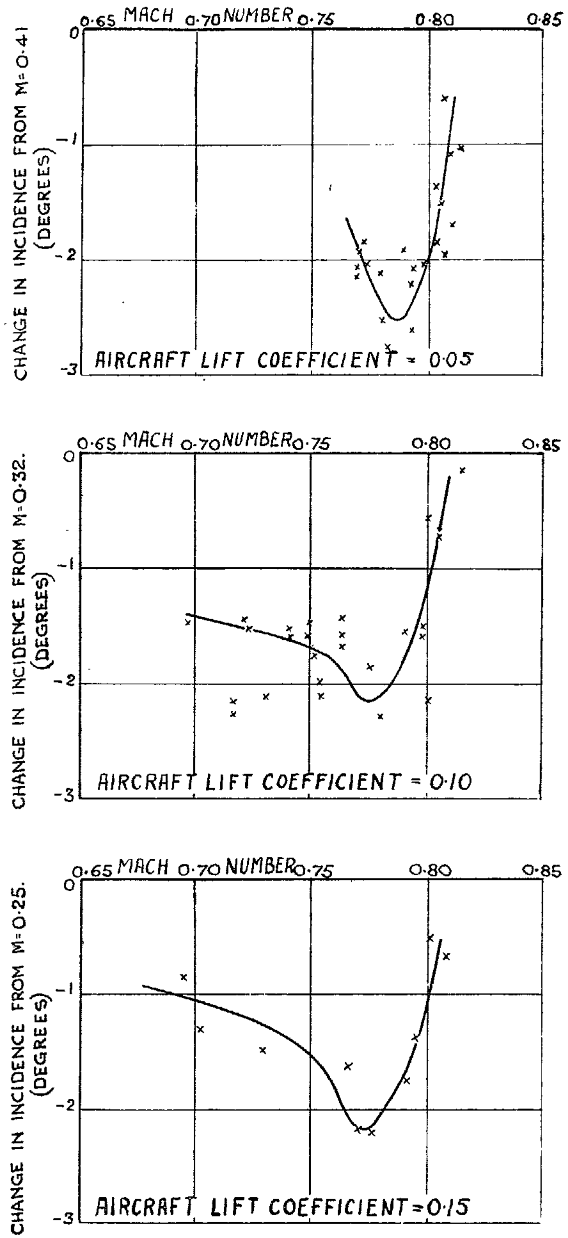

FIG. 9. Incidence Measured at Starboard Wing Tip.

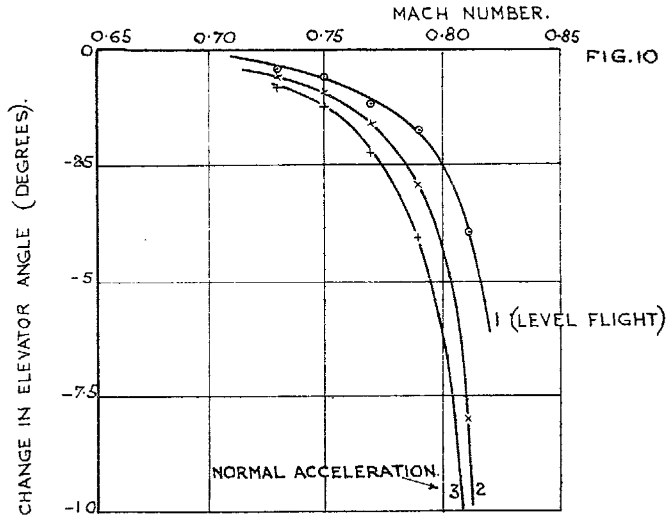

FIG. 10. Change of Elevator Angle.

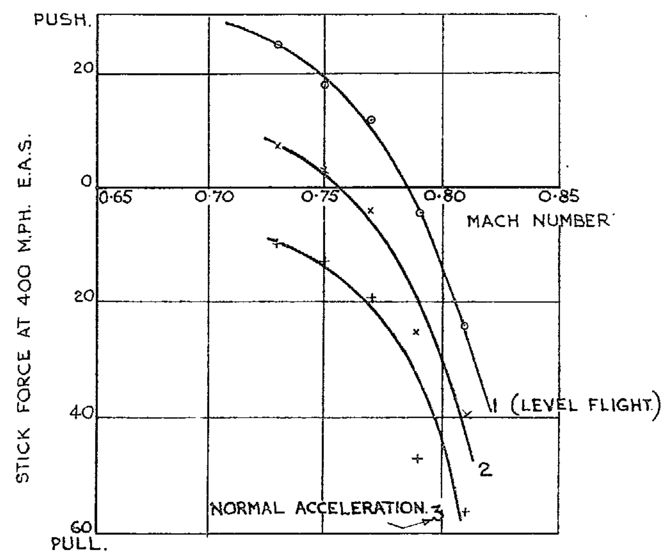

FIG. 11. Stick Force at 400 m.p.h. E.A.S.

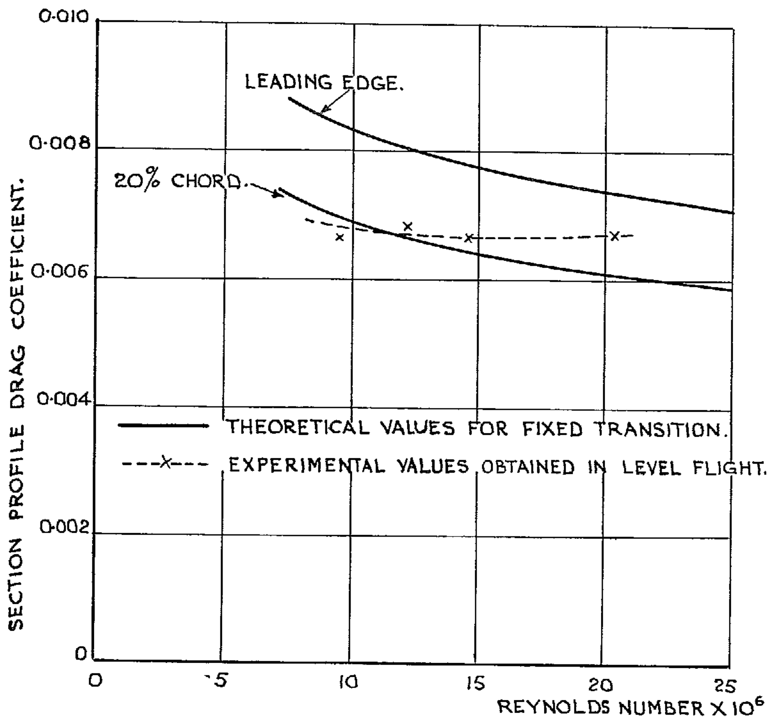

FIG. 12. Section Profile Drag Coefficient at Low Mach Number.

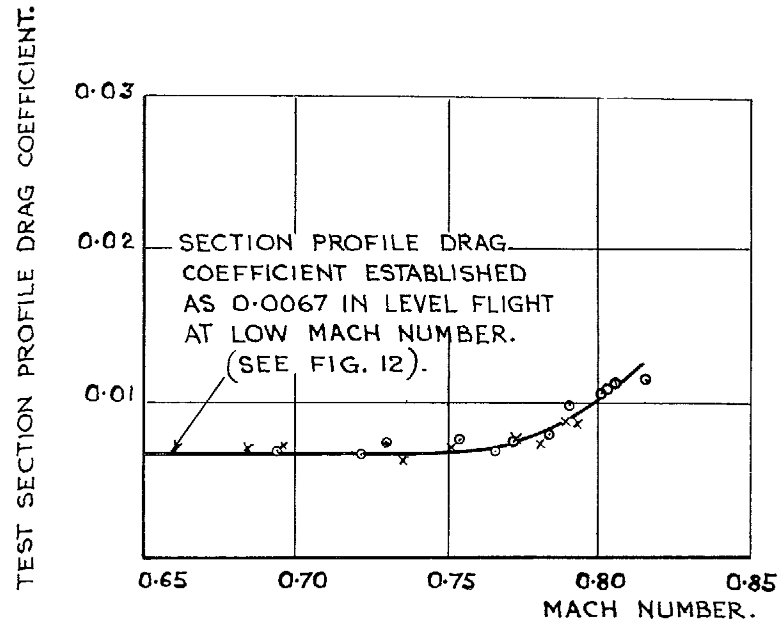

FIG. 13. Section Profile Drag Coefficient Excluding Shock Wave Drag.

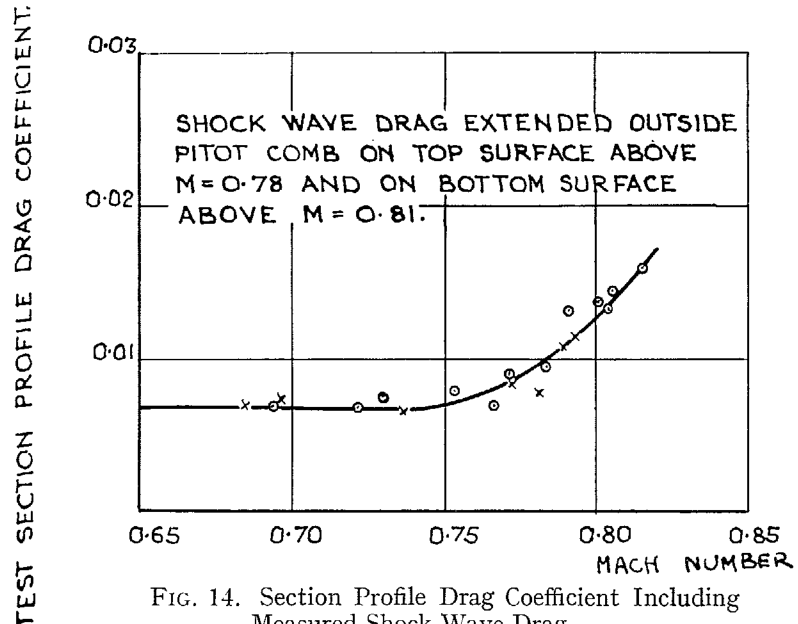

FIG. 14. Section Profile Drag Coefficient Including Measured Shock Wave Drag.

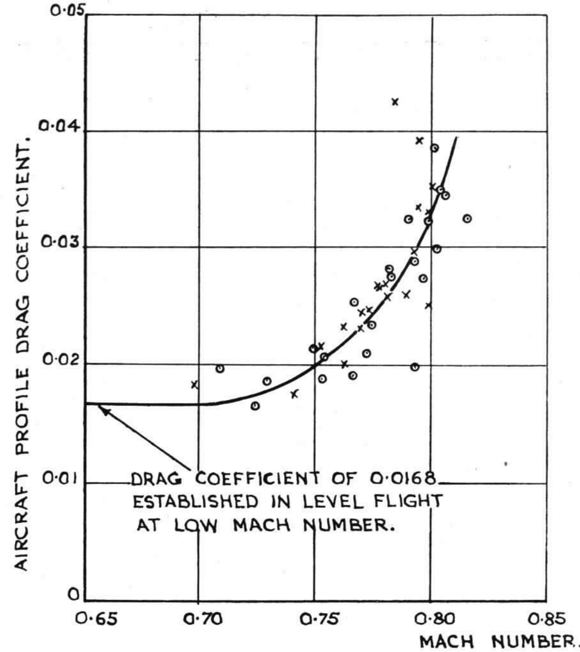

FIG. 15. Aircraft Drag Coefficient

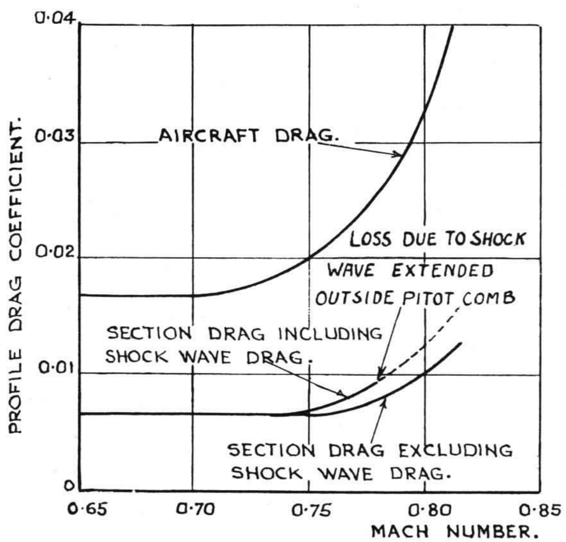

FIG. 16. Comparison of Aircraft and Test Section Profile Drag Coefficients.

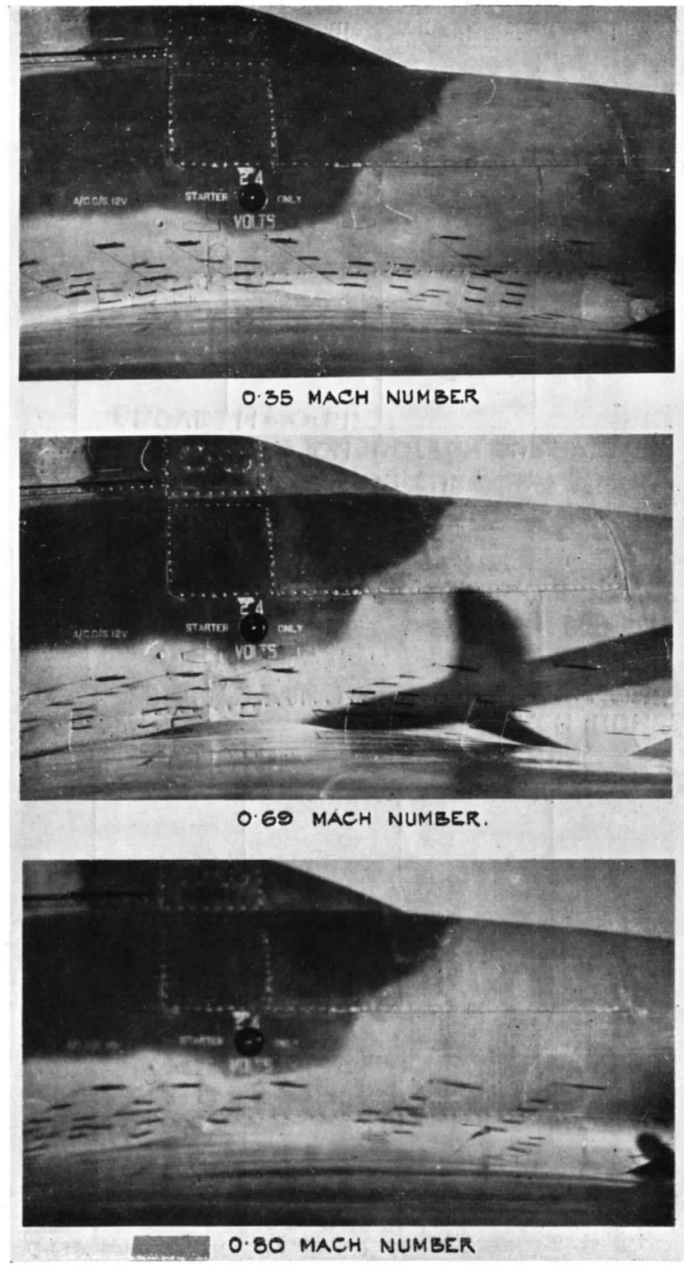

FIG. 17. Wing Root Tufts.

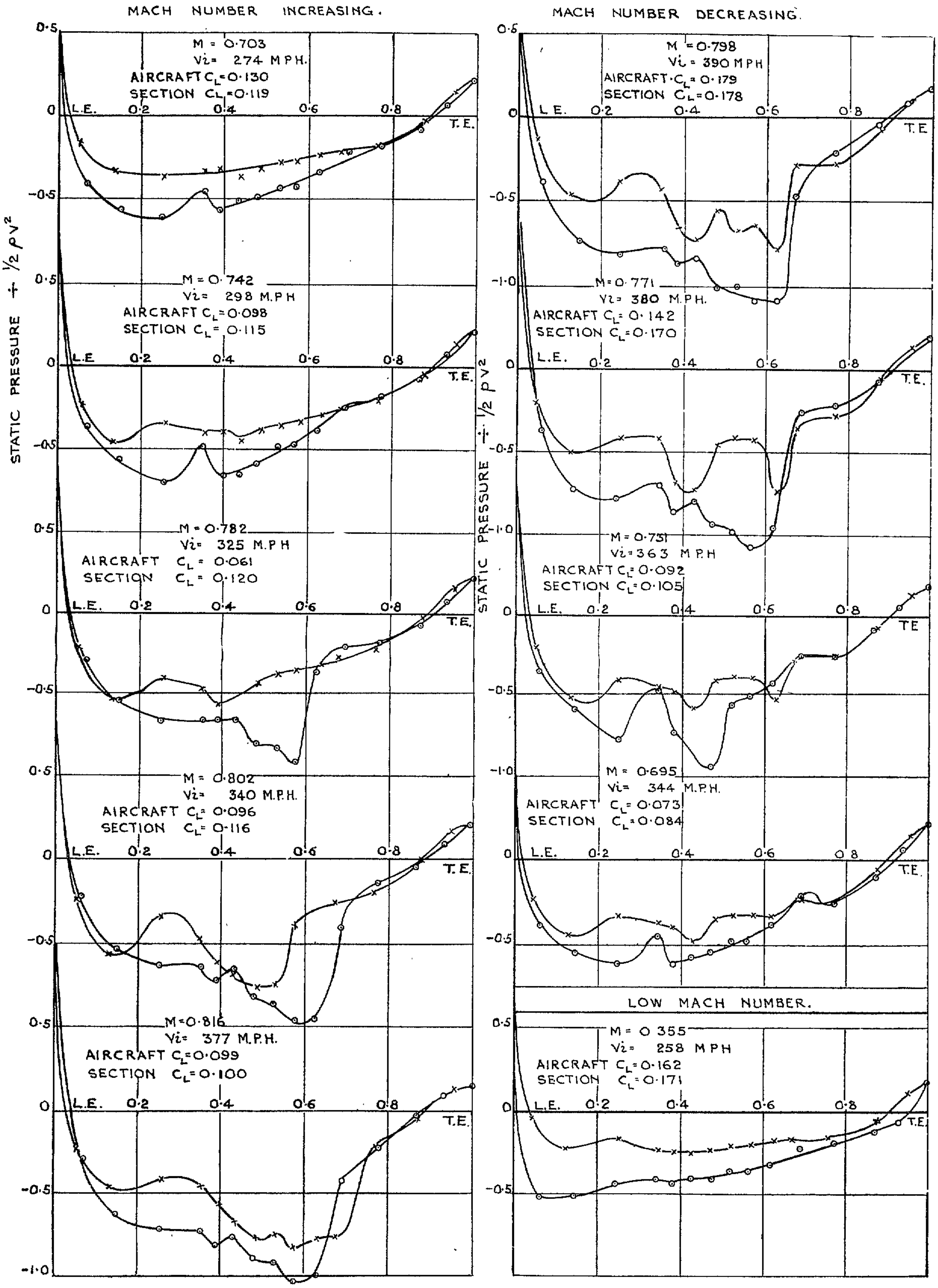

FIG 18. Test Section Pressure Distribution as Measured in Flight.

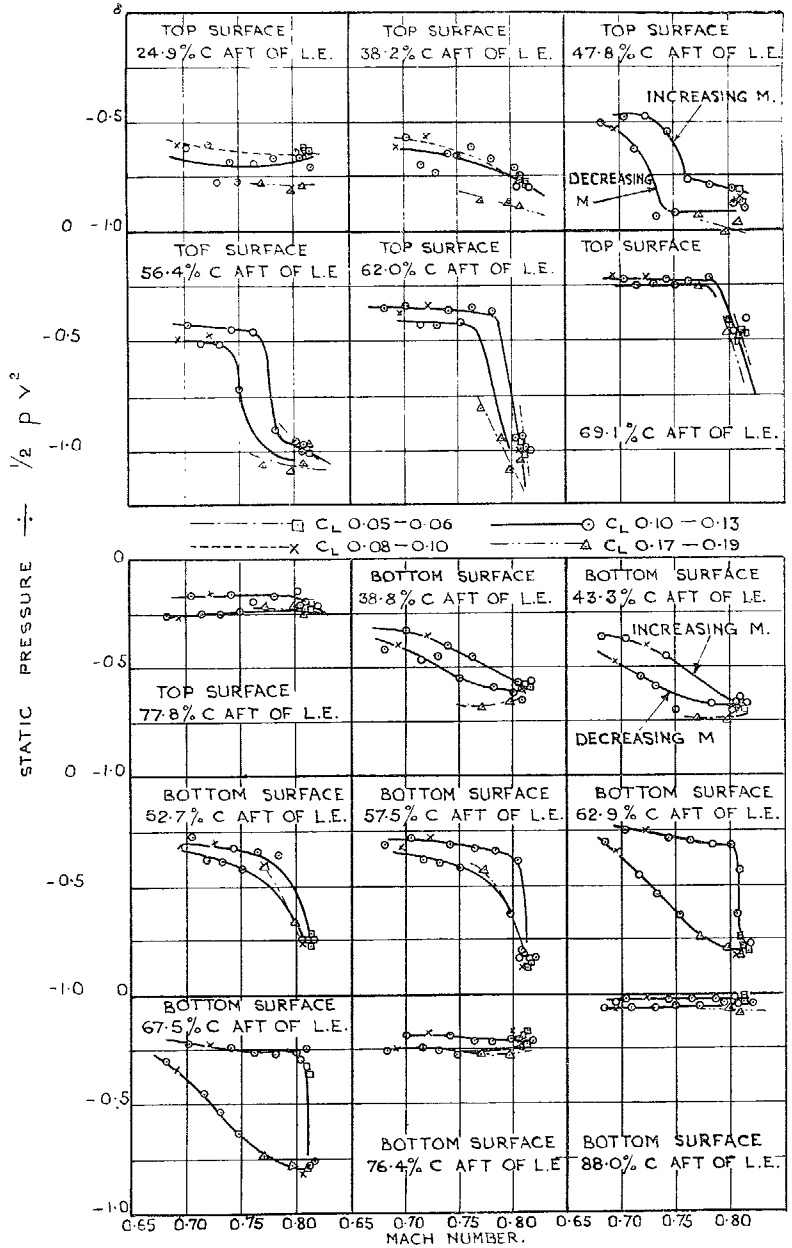

FIG. 19. Variation of Surface Pressure with Mach Number.

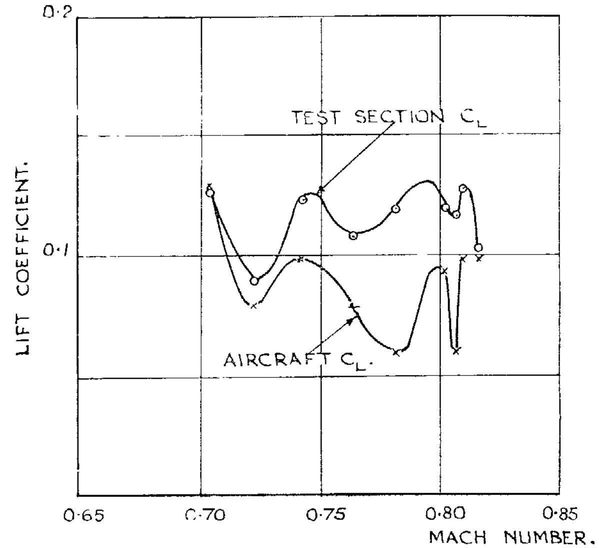

FIG. 20. Aircraft and Test Section Lift Coefficients.

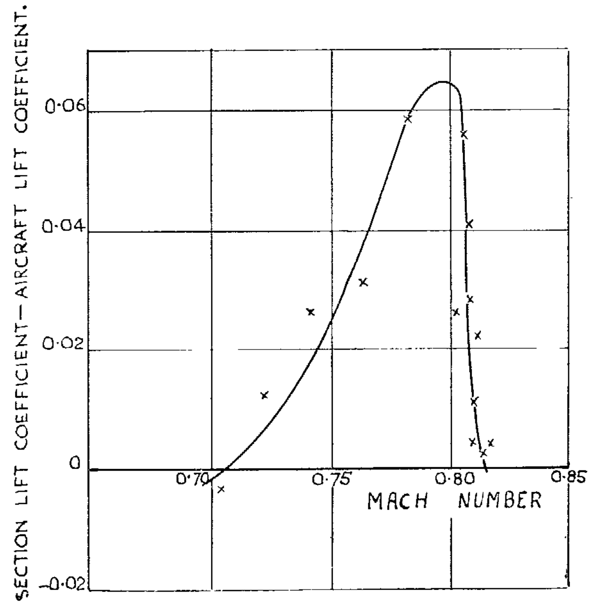

FIG. 21. Increase of Test Section Lift Coefficient over Aircraft Lift Coefficient.

(85630) Wt.12/818 12/48 Hw.

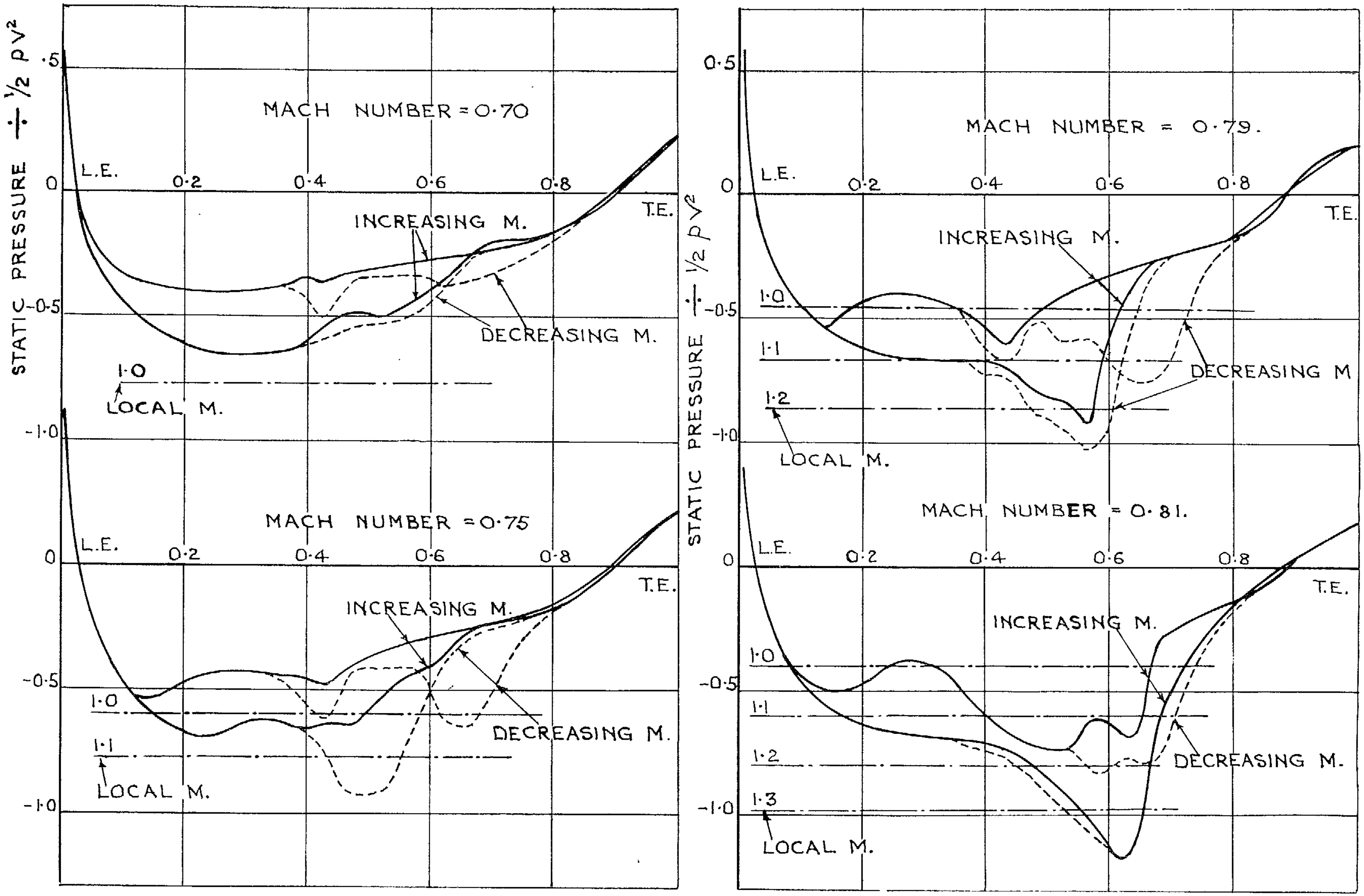

FIG. 22. Test Section Pressure Distribution Interpolated at Aircraft Lift Coefficient = 0·11.

PRINTED IN GREAT BRITAIN

S.O. Code No. 23-2264